Cooperative Mobile Positioning and Tracking in Hybrid WiMAX/WLAN Networks

Group No. 07gr1114

Francescantonio Della Rosa

June 2007

AALBORG UNIVERSITY

Aalborg University

E-Studyboard

Mobile Communications Master Thesis

TITLE:

Cooperative Mobile Positioning and Tracking in Hybrid WiMAX/WLAN Networks

THEME:

Mobile Communication

PROJECT PERIOD:

1st February 2007 - 7th June 2007

PROJECT GROUP:

07gr1114

GROUP MEMBERS:

Francescantonio Della Rosa

SUPERVISORS:

Simone Frattasi

João Figueiras

Number Of Duplicates:3

Number Of Pages In Report:51

Total Number Of Pages:60

Abstract

With the Cooperative Mobile Positioning (COMET) project we have started investigations in connection with the fourth generation (4G) with the purposes of designing an "augmentation" solution that could overcome the issues regarding GPS and GPS-free technologies in order to offer localization to anyone, anytime and anywhere. The idea behind the COMET originates from the fact that more likely reliable RSS measurements detected among neighboring mobiles can enhance the localization accuracy also in environments where usual terrestrial-based localization techniques offer a bad estimation.

For these purposes we have implemented an hybrid Mobile WiMAX / WLAN scenario where a data fusion for the position estimate is performed by the Extended Kalman Filter. Results obtained from the static and mobile case show that cooperation can enhance the location accuracy, offering more than 26 % of gain.

Acknowledgement

List of Abbreviations

3GPP	3rd Generation Partnership Project
AOA	Angle of Arrival
AWGN	Additive White Gaussian Noise
BS	Base Station
BWA	Broadband Wireless Access
DSL	Digital Subscriber Line
FDD	Frequency Division Duplex
GCC	Generalized Cross Correlation
GPS	Global Positioning System
GSM	Global System for Mobile Communications
HIPERMAN	HIgh PErformance Radio Metropolitan Area Network
HUMAN	High-speed Unlicensed Metropolitan Area Network
IEEE	Institute of Electrical and Electronics Engineers
LOS	Line Of Sight
MAC	Medium Access Control
MAN	Metropolitan Area Network
MIMO	Multiple Input Multiple Output
MMSE	Minimum Mean Square Error
MS	Mobile Station

NLOS	Non Line Of Sight
OFDM	Orthogonal Frequency Division Multiplexing
OFDMA	Orthogonal Frequency Division Multiple Access
PAN	Personal Area Network
PDP	Power Delay Profile
PHY	Physical Layer
RMSE	Root Mean Square Error
RS	Relay Station
RSS	Received Signal Strength
SC	Single Carrier
SNR	Signal to Noise Ratio
SOFDMA	Scalable Orthogonal Frequency Division Multiple Access
SP	Service Provider
SSA	small scale averaged
TDD	Time Division Duplex
TDMA	Time Division Multiple Access
TDOA	Time Difference of Arrival
TOA	Time of Arrival
WAN	Wide Area Network
Wi-Fi	Wireless Fidelity
WiMAX	Worldwide Interoperability for Microwave Access
WLAN	Wireless Local Area Network
WMAN	Wireless Metropolitan Area Network

Contents

List of Figures

List of Tables

Chapter 1

INTRODUCTION

Localization in cellular networks represents a great interest and a major importance for society and industry. Indeed, it can be used in many applications such as emergency, security, tracking, monitoring, intelligent transportation systems, mobile yellow pages, and cellular system management [1].

The most popular commercial solution reliable on the market to get accurate location information is the Global Positioning System (GPS), where time of arrival (TOA) measurements are calculated to provide the localization service. However, the introduction of mobile handsets with built-in GPS receivers in the third generation (3G) has led to an increased cost, size, battery consumption, and a long time for a full market penetration [1]. Moreover, not always the GPS is the most suitable solution for localization. The main drawback is represented by severely handicapped environments, such as outdoor urban canyons and indoor environments, which actually represent the greatest interest of service providers. In these conditions it is difficult, if not impossible, to obtain any sort of location information.
This is due to the infeasibility of having a clear view of at least four satellites, or due to signal blocking and multipath conditions [1].

The same drawback characterizes actual terrestrial-based (GPS-free) technologies when they are implemented in multipath environments and in non-line-of-sight conditions, specifically when no costly accurate environmental information is available. Hence, investigations have started in connection with the incoming fourth generation (4G) in order to design an "augmentation" solution a global solution useful to overcome the drawbacks of the GPS and the GPS-free technologies.

An alternative solution to do localization in long-range technology, such as in 3G, is by using time difference of arrival (TDOA) [2] which can be performed by using the same infrastructure for voice or data. Since TDOA does not need synchronization in terms of time with the transmitter, it does not need hardware modifications on the user device.

For picocells or short-range networks, such as Wireless Local Area Network (WLAN),

the positioning technique which is received signal strength (RSS)-based, depends on the received power. Because of the short distance between MSs TDOA is not suitable in this case, because a small error in TDOA can cause a great distance error compared to the distance between them.

When localization is done in cellular networks, the accuracy is highly dependent on the channel and line of sight (LOS) conditions. In some cases, due to the channel conditions poor results are obtained.

A novel solution to increase the localization accuracy in cellular networks is proposed by exploiting both long-range and short-range technologies. This can be done by cooperation between users using $ad - hoc$ communication in short range, exchanging their location information which is embedded in the received power.

Using transmission powers that are just large enough to ensure network connectivity, the ad-hoc network model achieves several performance benefits over the cellular one, including better spatial reuse characteristics and lower energy consumption [3]. It is straightforward to realize that a hybrid network model, such as the cellular ad-hoc one, is the most natural type of environment in which cooperation not only between users or terminals, but also between networks can be established and best exploited (we refer to this network model as the ad-coop network model).

The problem is to estimate the position of a user in a cellular network based on the observation of TDOA and RSS. Thus, a data fusion algorithm is required.

With the incoming of 4G, the need to define a polyvalent solution based on heterogeneous communication technologies is increasing. Moreover, there is a real need of providing an accurate location information *anytime anywhere.* [1].

Mobile Worldwide Interoperability for Microwave Access (WiMAX) is a good candidate for long-range technologies in 4G. It provides high data rates and flexibility in accessing the network anytime and anywhere, with less investments for the infrastructure. It can be operated in the unlicensed or licensed bands with a lower deployment cost with respect to 3G systems. [4]. A key advantage of WiMAX over other Wireless Metropolitan Area Network (WMAN) technologies is that it offers a single standard approach that do not rely on vendor specific proprietary solutions [5]. This means that manufacturers will take advantage of economies of scale, while operators will have a wider range of choice. Finally, the emergence of Mobile WiMAX, which allows interoperability and benefits for other technologies seems to point towards the 4G goals. Thus, WiMAX is a strong candidate to be the standard of the next generation mobile technology [6]. Based on [6], it seems that WiMAX is not intended to replace WLAN, but rather to complement it. Thus, the cooperation between them can be implemented. Additionally, localization can be introduced in these technologies to enrich the number of services, using the methods mentioned above.

In this thesis, a method of cooperation to perform the localization service in a system based on the coexistence of these two technologies is proposed. WiMAX is used as the cellular network and WLAN is as the $ad - hoc$ network model.

Chapter 2

PROJECT DESCRIPTION

2.1   Introduction

The purpose of the this project is to enhance the localization accuracy in cellular systems for moving GPS-free portable devices in outdoor scenarios. While traditional localization techniques for cellular networks make use of TOA/AOA and TDOA measurements, we try to improve the estimate of the users' positions by also exchanging RSS measurements. This exchange can be done by forming an *ad-hoc* network among mobile stations (MSs). As a consequence, a must is that the distance among MSs must be small enough to form an *ad-hoc* network. The core of the technique implemented is represented by the fusion of the data obtained from the long- (BS-MS) and short-range (MS-MS) measurements.

2.2   Scenario

The results in this work are obtained by simulations implemented in Matlab, where a hybrid Mobile WiMAX / WLAN 802.11a system is simulated in an outdoor scenario. The scenario (see Fig. 2.1) is defined as follows:

- Long-range - Mobile WiMAX (IEEE 802.16e): four BSs are assumed; two MSs are positioned in the cell where the reference BS (i.e. BS1) is located. All MSs receive preamble signals coming from four BSs and perform cross-correlation; NLOS conditions are taken into account for BSs-MSs links.

- Short-range - WLAN (IEEE 802.11a): two MSs are assumed; MSs are connected in ad-hoc mode, and exchange RSS information; LOS conditions are considered on this link.

- Motion Model: first a static case is evaluated, then pedestrian mobility is introduced for cooperating MSs.
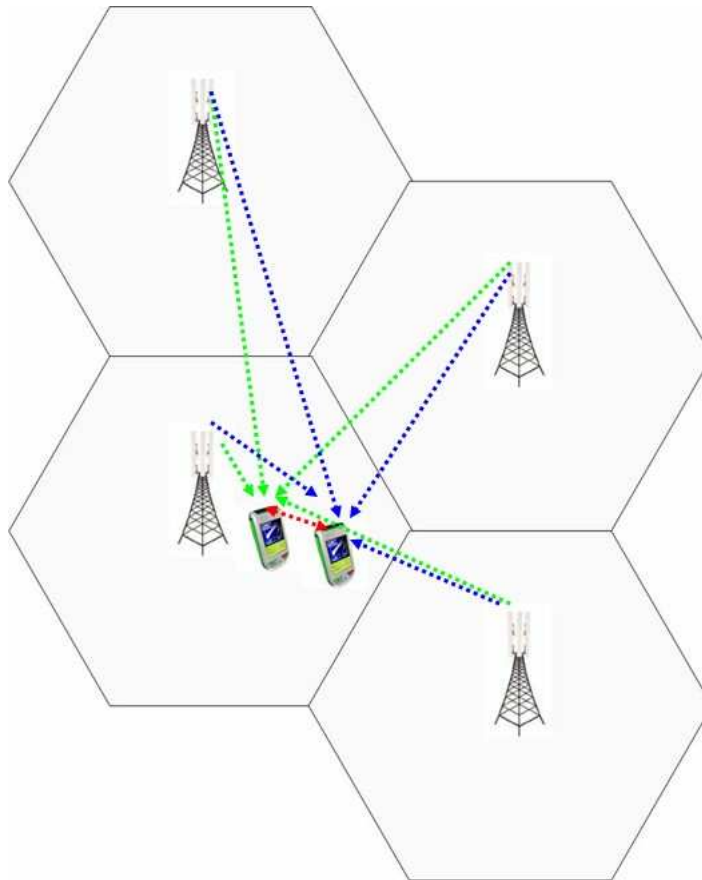
Figure 2.1: Illustration of the reference scenario.

2.3   Problem Definition

In a cellular scenario the positioning functionality is provided by making use of the radio signals to determine the geographical location of the MS. Clients associated with the MS or attached to the core network may request the location information. This information may be used internally by the cellular network for providing value-added network services, by the MS itself or by "third party" service providers (SPs).

In this report, two different types of technologies are exploited to enhance the accuracy of the localization. In Mobile WiMAX the position of an MS is estimated by using the TDOA technique. The WLAN 802.11a will be instead used to get the RSS information. Then, the data fusion will be performed to combine the measurements and improve the accuracy.

2.4   Scope of the Project

The purpose of this project is to provide a solution to enhance the localization accuracy when tracking users' in hybrid WiMAX / Wi-Fi networks by exploiting location info both in long-range and short-range links. The key point of this work is the cooperation among mobiles. Basically in this report we design a data fusion implemented by the Extended Kalman Filter (EKF).

The following list summarizes the aims of the project:

- To study and analyze localization techniques in cellular *ad-hoc* networks.

- To study and analyze the Mobile WiMAX and the WLAN 802.11a technology.

- To study and describe the filtering technique used as data fusion.

- To propose a novel technique able to enhance the localization accuracy in 4G cellular networks.

2.5   Assumptions

Some assumptions are needed in order to manage the complexity of the problem proposed in this thesis and to have a more focussed attention on the localization problem.

- All MSs are connected to the same BS (the reference BS) and located in the same cell.

- All the MSs are in LOS with each other and NLOS with the BSs.

- Handover is not taken into account.

- Omnidirectional antennas are used in every cell.

- Shadowing is not considered.

Chapter 3

BACKGROUND THEORY

3.1 Fundamentals of positioning

3.1.1 Positioning Techniques

In this section, a collection of positioning techniques is shown. All these techniques represent the basis of the localization process, since they are needed to track the trajectory of users in a cellular system [7]. An important issue is where the data is processed. Based on that, we make te following classification [7]:

Network-Based: measurements and computation of a location position estimate are performed by BSs in the network.

Mobile-Based: measurements and computation of a location position estimate are performed by MSs.

Mobile-Assisted: MSs provide position measurements to the network, which will perform computations for location estimate. Additionally, techniques for localizations are mentioned below:

- *AOA technique*: AOA information can be obtained by using antenna arrays. The drawbacks of this method are the need of extra hardware (antenna arrays at the BSs), and the need for LOS conditions for better accuracy.

- *TOA technique*: TOA information, either in uplink or in downlink, can be obained in many ways. If the user device and the BS are synchronized, TOA can be calculated to get the distance between them. The drawback of this technique is that it requires a very accurate timing reference between the clocks of the MS and the BSs. Another way to calculate TOA is by determining the time that the signal takes on the forward link (downlink) or the reverse link (uplink). This can be done by measuring the time in which the user responds to an instruction transmitted from the BS. The total elapsed time is composed of the sum of the round trip signal delay and any processing

and response delay of the user device. Half of that quantity is the estimation of the signal delay in one direction, which would give the approximate distance of the user device from the BS.

- *TDOA technique*: TDOA information can be obtained by estimating the difference in the arrival times of the signal from the source at multiple receivers. In the uplink case, this is usually accomplished by taking a snapshot of the received signal at different BSs by assuming that they are synchronized in time. In the downlink case, several BSs that are assumed to be synchronized with each other (e.g. via GPS equipment), send the signal to the MS. Then, the MS performs the cross-correlation of the two versions of the signal coming from two different BSs and the peak of the cross-correlation output gives the TDOA. A particular value of the time difference estimate defines an hyperbola between the two receivers on which the mobile may be located, assuming that the source and the receivers are coplanar. The hyperboloid is defined as a surface and has a constant distance difference from the two points. If this procedure is done for other BSs, another hyperbola is defined in order to estimate the position location. This method is also called *hyperbolic position method*. One of the benefit of this technique is that it does not require knowledge of the absolute time of the transmission. The required changes to incorporate the TDOA method are only in the software of the system. *Note that for such benefit the TDOA is the technique we will focus on.*

3.1.2 TDOA Measurements

TDOA measurements can be estimated by performing the cross-correlation between two received signals [8]. In this project, the TDOA calculation is assumed to be done in downlink. For each assumed position, both in static and mobile case, the received signals can be expressed by the following equations :

$$\begin{aligned} x_1(t) &= A_1 s(t - d_1) + n_1(t) \\ x_2(t) &= A_2 s(t - d_2) + n_2(t) \end{aligned} \tag{3.1}$$

where $x_1(t)$ and $x_2(t)$ represent the arriving signals at MS from BS1 and BS2, A_1 and A_2 are the amplitudes of the signals, $s(t)$ is the source signal, $n_1(t)$ and $n_2(t)$ are additive noises, and d_1 and d_2 are signal arrival times at MS from BS1 and BS2. An assumption of the model is that $s(t)$, $n_1(t)$, and $n_2(t)$ are zero-mean random process, real and jointly stationary, and uncorrelated with each other.

Without losing of generality, assuming $d_1 < d_2$, the equations can be derived as follows:
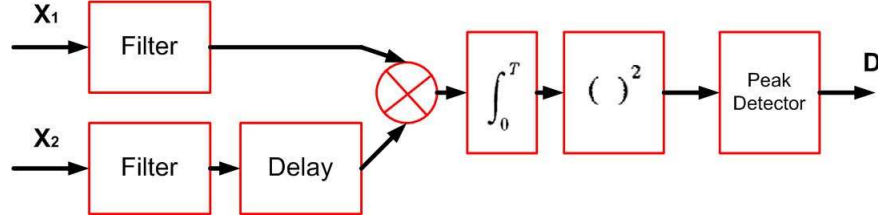
Figure 3.1: Illustration of TDOA estimation by using GCC.

$$x_1(t) = s(t) + n_1(t)$$
$$x_2(t) = As(t + D) + n_2(t) \quad (3.2)$$
$$D = d_2 - d_1$$

where A is the received signal amplitude ratio between BS1 and BS2, and D represents the TDOA. The TDOA estimation of s_t is derived from the generalized cross correlation (GCC) equation (Fig. 3.1):

$$R_{x_1 x_2}(\tau) = E[x_1(t) x_2(t - \tau)] \quad (3.3)$$

$R_{x_1 x_2}$ represents the cross-correlation between the signals x_1 and x_2, and E denotes the expectation. The estimate of the delay is provided by the argument τ, which is the parameter that maximizes $R_{x_1 x_2}$. In addition, $R_{x_1 x_2}$ can only be estimated because of finite observation time:

$$\overline{R}_{x_1 x_2}(\tau) = \frac{1}{T} \int_0^T x_1(t) x_2(t - \tau) dt \quad (3.4)$$

where $\overline{R}_{x_1 x_2}(\tau)$ is an estimate of the cross-correlation, and T represents the observation interval.

3.1.3 RSS Measurements

For the short-range link between MSs, the technique that can be used for estimating the position is based on RSS. This technique is related to the received power at an MS, which is used to calculate the predicted distance by means of a certain pathloss model. Note that the TDOA technique cannot be applied because the distances between MSs are so small that small errors in TDOA estimations would give huge errors when estimating their positions.

3.2   Data Fusion

The data fusion proposed in this work is adopted to combine TDOA measurements with RSS measurements, in order to enhance the localization accuracy of the system. In this section, a detailed description of the theory behind the implemented method will be given. The EKF represents the core of the implementation. This type of filter is actually the most used to perform positioning and tracking.

3.2.1   The Filtering Problem

A particular branch of filter theory focuses on an optimum criterion for the estimate of the filtered signal: minimum mean square error (MMSE) criterion [9]. This branch of filter there was with N. Wiener's work in the 1940s [10] when he began to adopt the knowledge of the past input value to estimate the current output value. Wiener's filter is based on specific statistical parameters that limit MS applicability, thus it is often not practically achievable [9].

Some years later, in 1960, a new approach to linear filtering and prediction problems has been proposed by R. E. Kalman: the use of the recursive state space methods [11]. This approach is founded on the estimate over the state space of a dynamic system that bases itself on previous noisy measurements done in the system. [1]

Some probabilistic models of the system are required to apply this method: the *motion model*, that describes the system dynamics, and the *perceptual model* related to the noisy observations of the state.

3.2.2   The Filtering Technique

In a dynamic system the state is represented by a vector $x_k \in R^n$. The index k indicates the process time and is characterized by the following probabilistic model:

$$x_k = f_{k-1}(x_{k-1}, w_{k-1}) \tag{3.5}$$

As it can be observed, the state at time k is a function of the state at the previous time $k-1$ and the noise sequence w_{k-1} at time $k-1$ as well. The state vector estimation is based on observations made on the system that are stored in another vector $Z_k = \{z_i, i = 0, ..., k\}$, where z_i is the measurement obtained at time i. Obviously, the observation vector is a function of the state:

$$z_k = h_k(x_k, v_k) \tag{3.6}$$

---

[1] To understand more about the history of the filter theory more information can be found in [12].

where v_k is the noise sequence that affects the estimate of the state. Both the noise sequences, w_{k-1} and v_k are considered to be individually and mutually independent and with a given probability density function (pdf) [9].

The purpose of the Bayes filter is the setting-up of the posterior probability density function $p(x_k|Z_k)$, also called *belief* [13]. The *belief* is achievable by a recursive algorithm by capturing the measurements Z_k. First the algorithm supposes the knowledge of the statistic of the initial state when no measurements are considered:

$$p(x_0) = p(x_0|z_0), \tag{3.7}$$

evolving later on in two progressive steps: the *prediction* stage and the *update* stage.

The prediction stage starts assuming that the pdf $p(x_{k-1}|Z_{k-1})$ is known at time $k-1$. The procedure continues with the calculation of the prediction density function at time k based on all the measurement available at time $k-1$, i.e., Z_{k-1}:

$$p(x_k|Z_{k-1}) = \int p(x_k|x_{k-1})p(x_{k-1}|Z_{k-1})\,dx_{k-1} \tag{3.8}$$

$$= \int p(x_k|x_{k-1}, Z_{k-1})p(x_{k-1}|Z_{k-1})\,dx_{k-1} \tag{3.9}$$

$$\tag{3.10}$$

In the above formula a first order Markov process $[p(x_k|x_{k-1}, Z_{k-1}) = p(x_k|x_{k-1})]$ has been adopted [9]. The update stage starts when the new observation at time k, z_k, is ready to be processed. Thus,the algorithm calculates the posterior probability function using the Bayes' law after updating the previous prediction density.

$$p(x_k|z_k) = p(x_k|z_k, z_{k-1}) \tag{3.11}$$

$$= \frac{p(z_k|x_k, z_{k-1})p(x_k|z_{k-1})}{p(z_k|z_{k-1})} \tag{3.12}$$

$$= \frac{p(z_k|x_k)p(x_k|z_{k-1})}{p(z_k|z_{k-1})} \tag{3.13}$$

where the denominator in the formula depends on:

$$p(z_k|Z_{k-1}) = \int p(z_k|x_k)p(x_k|Z_{k-1})\,dx_k \tag{3.14}$$

At this point any criteria is applicable to estimate the state vector in an optimum way. Usually, as it has been mentioned in the introduction, the optimum criterion adopted is the MMSE criteria.

3.2.3 Introduction to the Kalman Filter

Some assumptions on the probability density function $p(x_k|Z_k)$ explained before determine a different Bayesian filtering approach and a different algorithm. If the Belief follows a

Gaussian distribution the filter becomes the Kalman filter. In that case, at each time k, the posterior probability density is considered to be Gaussian and it is completely characterized by knowing its first and second moment, the mean and the covariance.

Below we mention some key issues regarding the Kalman filter:

- In the state model Eq. (4.1), the function f_{k-1} is linear function of the state x_{k-1} and the noise vector w_{k-1};

- In the observation model Eq. (4.2), the function h_k is a linear function of the state x_k and the noise vector v_k;

- The elements of the noise vectors w_{k-1} and v_k are Gaussian random variables, zero-mean and with covariance matrices Q and R:

$$p(w) \quad \sim \quad N(0, Q) \tag{3.15}$$
$$p(v) \quad \sim \quad N(0, R) \tag{3.16}$$
$$\tag{3.17}$$

With these assumptions it is obtained the following linear stochastic difference equations:

$$x_k \quad = \quad Ax_{k-1} + Bu_{k-1} + w_{k-1} \tag{3.18}$$
$$z_k \quad = \quad Hx_k + v_k \tag{3.19}$$
$$\tag{3.20}$$

where A is a $n \times n$ matrix, called transition matrix, that correlate the state x_k at time k with the state x_{k-1} at time $k-1$. The random variable $u \in R^l$ represents the optional control input and B is a $n \times l$ matrix that relates the current state x_k to the control input u_{k-1} at time $k-1$. Finally, H is a matrix $m \times n$ that defines the linear relationship between the measurement vector z_k and the state x_k at same time k. To be noted that, in general, the matrices A, B, H relate to the state and the observation model, and the covariance matrices of the noise vectors Q and R are variant in time and depending on the application [14].

Some definitions are now necessary to explain the steps of the Kalman algorithm. The prior state estimate $\hat{x}_k^- \in R^n$ indicates the estimation of the state vector x_k at time k when all the observations Z_{k-1} obtained until time $k-1$ are taken into account. Indeed, the posterior state estimate $\hat{x}_k \in R^n$ represents the estimation of the state vector obtained at time k when the observation z_k is available. All estimations are supposed to be optimum according to the MMSE criterion. It is defined prior estimate error the difference between the real value of the state vector and the prior state estimate:

$$\hat{e}_k^- = x_k - \hat{x}_k^- \tag{3.21}$$

13

and the posterior estimate error the difference between the real value of the state vector and the posterior state estimate:

$$\hat{e}_k = x_k - \hat{x}_k \qquad (3.22)$$

In the same way, it is possible to define the prior and posterior estimate error covariance:

$$P_k^- = E[\hat{e}_k^- \hat{e}_k^{-T}] \qquad (3.23)$$
$$P_k = E[\hat{e}_k \hat{e}_k^T] \qquad (3.24)$$
$$\qquad (3.25)$$

As previously mentioned, to run the Kalman filter is enough to know the first and second moment of the *belief*:

$$\hat{x}_k = E[x_k] \qquad (3.26)$$
$$P_k = E[(x_k - \hat{x}_k)(x_k - \hat{x}_k)^T] \qquad (3.27)$$
$$\qquad (3.28)$$

Therefore the posterior density function is distributed as

$$p(x_k|z_k) \sim N(E[x_k], E[(x_k - \hat{x}_k)(x_k - \hat{x}_k)^T]) \equiv N(\hat{x}_k, P_k) \qquad (3.29)$$

The Kalman algorithm requires the knowledge of the initial state estimate $\hat{x}_{k=0}$ and the initial estimate error covariance $P_{k=0}$.

When the first observation z_1 is available, the algorithm estimates $\hat{x}_1$ with the constraint that the posterior estimate error covariance P_1 is minimum (MMSE criterion), and so forth with the next step.

Since the Kalman algorithm corrects the previous estimate by using a feedback [14], supposing of being at step $k - 1$ and of knowing the posterior state estimate $\hat{x}_{k-1}$ and its posterior estimate error covariance P_{k-1}, the algorithm evolves in two distinct stages: *prediction* stage and *update* stage.

In the prediction stage the aim is to find $\hat{x}_k^-$ according to all the measurements available Z_{k-1}. Later it calculates the prior estimate error covariance P_k^-. The equations representing the algorithm are listed below:

$$\hat{x}_k^- = A\hat{x}_{k-1} + Bu_{k-1} \qquad (3.30)$$
$$P_k^- = AP_{k-1}A^T + Q_{k-1} \qquad (3.31)$$
$$\qquad (3.32)$$

In the update stage first of all the Kalman gain K_k or blending factor is computed. It represents the gain that minimizes the posterior covariance:

$$K_k = P_k^- H^T S^{-1} = P_k^- H^T (H_k P_k^- H_k^T + R_k)^{-1} \tag{3.33}$$

The next steps concern the computation of the posterior state estimate $\hat{x}_k$ by the capture of the current measurement z_k, and the posterior estimate error covariance P_k:

$$\hat{x}_k = \hat{x}_k^- + K_k(z_k - H\hat{x}_k^-) \tag{3.34}$$

$$P_k = (I - K_k H)P_k^- \tag{3.35}$$

$$\tag{3.36}$$

The different $(z_k - Hx_k^-)$ is called innovation process. It represents the innovation about the state x_k at time k thanks to the measurement z_k. It is called innovation or residual [14]. This new information is included in the Kalman gain formula, the matrix S , which is the covariance matrix of the difference $(z_k - Hx_k^-)$.

3.2.4 The Extended Kalman Filter

If the Kalman filter is applied with linear dynamic systems, a different solution has been studied when either the system dynamic model or the observation model are non-linear. The EKF is part of this category of non-linear filters [9].

In the EKF the equations that control the state model and the observation model are non linear stochastic difference equations. The form of the equations are still the same for both the state vector $x_k \in R^n$ and the observation vector $z_k \in R^n$:

$$x_k = f_{k-1}(x_{k-1}, u_{k-1}, w_{k-1}) \tag{3.37}$$

$$z_k = h_{k-1}(x_k, v_k) \tag{3.38}$$

where

- w_k: zero-mean process noise;

- v_k: zero-mean measurement noise;

- f: non-linear function that links the state at time *k-1* to the state at time k;

- u_k: optional control input;

- h: non-linear function that links the state at time k to the measurement at time k;

Although the values of w_k and v_k are unknown at each time step, it is still possible to approximate the state and the observation as follows:

$$\tilde{x}_k \ = \ f_{k-1}(x_{k-1}, u_{k-1}, 0) \tag{3.39}$$

$$\tilde{z}_k \ = \ h_k(x_k, 0) \tag{3.40}$$

$$\tag{3.41}$$

The core of the EKF is the linearization of the models:

$$x_k \approx \tilde{x}_k + A_{k-1}(x_{k-1} - \hat{x}_{k-1}, 0) + W_k w_{k-1} \tag{3.42}$$

$$z_k \approx \tilde{z}_k + H_k(x_k - \tilde{x}_k) + V_k v_k \tag{3.43}$$

where the parameters used are [14]:

- x_k: current state vector;

- z_k: current measurement vector;

- $\tilde{x}_k$: approximate state vector;

- $\tilde{z}_k$: approximate measurement vector;

- $\hat{x}_k$: posterior state estimate vector;

- w_k: random variable representing the process noise;

- v_k: random variable representing the measurement noise;

- $A_{[i,j],k-1} = \frac{\partial f_{[i],k-1}(x_{k-1}, u_{k-1}, 0)}{\partial x_{[j]}}$: the Jacobian matrix of partial derivatives of f with respect to x;

- $W_{[i,j],k-1} = \frac{\partial f_{[i],k-1}(x_{k-1}, u_{k-1}, 0)}{\partial w_{[j]}}$: the Jacobian matrix of partial derivatives of f with respect to w;

- $H_{[i,j],k} = \frac{\partial h_{[i],k}(\tilde{x}_k, 0)}{\partial x_{[j]}}$: the Jacobian matrix of partial derivatives of h with respect to x;

- $V_{[i,j],k} = \frac{\partial h_{[i],k}(\tilde{x}_k, 0)}{\partial v_{[j]}}$: the Jacobian matrix of partial derivatives of h with respect to v;

It is defined the error with respect to the state vector and the measurement vector as the difference between the true value and the approximated:

$$\tilde{e}_{x_k} \ \equiv \ x_k - \tilde{x}_k \tag{3.44}$$

$$\tilde{e}_{z_k} \ \equiv \ z_k - \tilde{z}_k \tag{3.45}$$

$$\tag{3.46}$$

Using the approximations 3.42 and 3.43 the above equations can be rewritten as:

$$\tilde{e}_{x_k} \approx A_{k-1}(x_{k-1} - \hat{x}_{k-1}) + \varepsilon_k \tag{3.47}$$

$$\tilde{e}_{z_k} \approx H_k \tilde{e}_{x_k} + \eta_k \tag{3.48}$$

$$\tag{3.49}$$

where

- ε_k: zero-mean random variable with covariance matrix WQW^T, and Q the covariance matrix of w_k;

- η_k: zero-mean random variable with covariance matrix VRV^T, and R the covariance matrix of v_k;

It can be noted that these equations are now linear because of the linearization of the system models. Then, the algorithm evolves estimating the prediction error $\tilde{e}_{x_k}$ by calculating:

$$\hat{e}_k = K_k \tilde{e}_{z_k} \tag{3.50}$$

Finally, the algorithm estimates the state vector as follows:

$$\hat{x_k} = \tilde{x}_k + \hat{e}_k = \tilde{x}_k + K_k \tilde{e}_{z_k} = \tilde{x}_k + K_k(z_k - \tilde{z}_k) \tag{3.51}$$

Now that all the equations characterizing the algorithm for the EKF are available it is possible to split them in *prediction* and *update* equations, as shown in Fig. 3.2.

3.3 OFDM Modulation Technique

Engineers have used Orthogonal Frequency Division Multiplexing (OFDM) in multiple broadband technology deployments such as digital TV in Europe, Japan, and Australia and Digital Subscriber Line (DSL) technology. OFDM devices use one frequency channel devided into several subchannels. Each of these subchannels are used to transmit data. Thus, the main function of OFDM is to encode a single channel into multiple subcarriers.

The OFDM technique was developed in order to avoid the waste of bandwidth that caused the old FDM. Indeed, the FDM technique gave to each user an exclusive channel and guard bands, which were used to ensure data do not interfere with one another. To avoid unused guard bands, OFDM selects channels that overlap but do not interfere with each other. Overlapping carriers are allowed because the subcarriers are defined so that they are easily distinguished from one another. The ability to separate the subcarriers lays on a complex mathematical relationship called *orthogonality*. Subcarriers are orthogonal
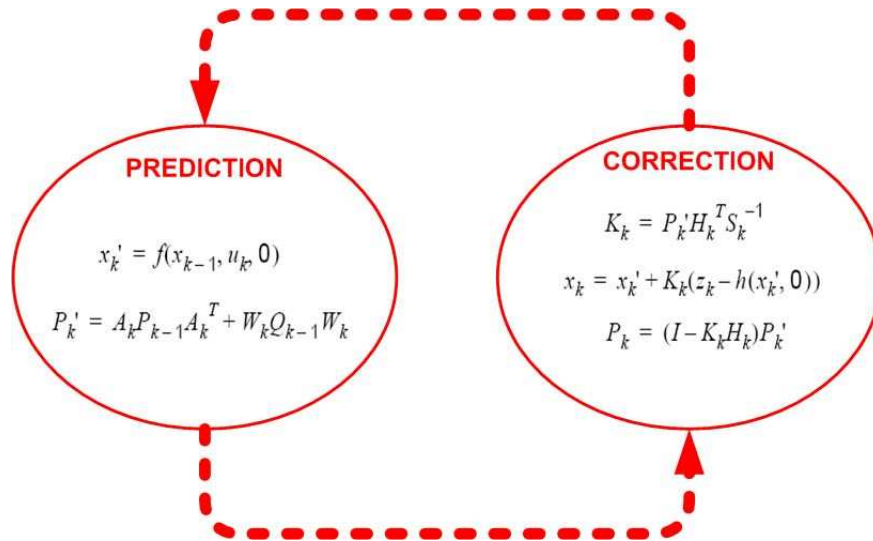
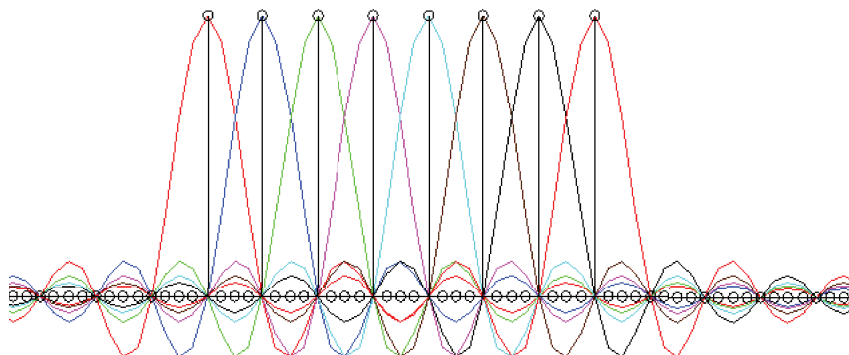Figure 3.2: An overview of the Extended Kalman filter algorithm [14]

Figure 3.3: Orthogonal frequency components

to each other: when the peak of one subcarrier appears, the other subcarriers have zero amplitude. The peak of each subcarrier encodes data (see Fig. 3.3)

As shown in Fig. 3.4 a serial-to-parallel buffer subdivides the information sequence into frames of several bits. OFDM allows to transmit a different number of bits/symbol on each subcarrier. The Inverse Fast Fourier Transform (IFFT) is used to create a composite waveform from the coded signal from each subchannel. OFDM receivers can then apply the Fast Fourier Transform (FFT) to a received waveform to extract the amplitude of each component subcarrier. The cyclic prefix for the block of samples avoids intersymbol interference [15].

OFDM is a proven technology providing high spectral efficiency, protecting against interference, and reducing multipath distortion [15].
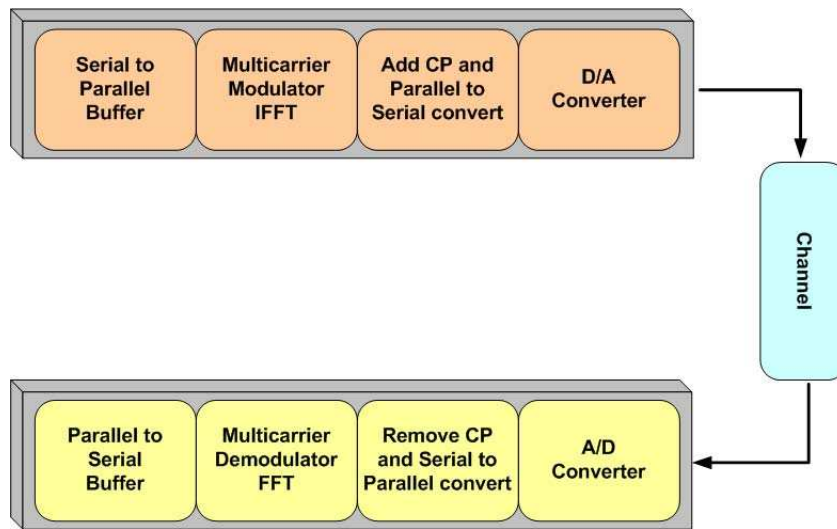
Figure 3.4: OFDM Block diagram

3.4   Channel Model

An important requirement to model wireless communication systems is to have an accurate description of the wireless channel. This description can act as a basis for performance evaluation and comparison. The-ever changing channel conditions heavily dependent upon the terrain, tree and building density, antenna height and other parameters. In general, it can be characterized by:

- Path loss;

- Shadowing;

- Small Scale Fading;

19

Fig. 3.5 shows the three main propagation characteristics that affect the wireless channel. Note that we do not take into account shadow fading.

Figure 3.5: Propagation characteristics in a wireless channel.

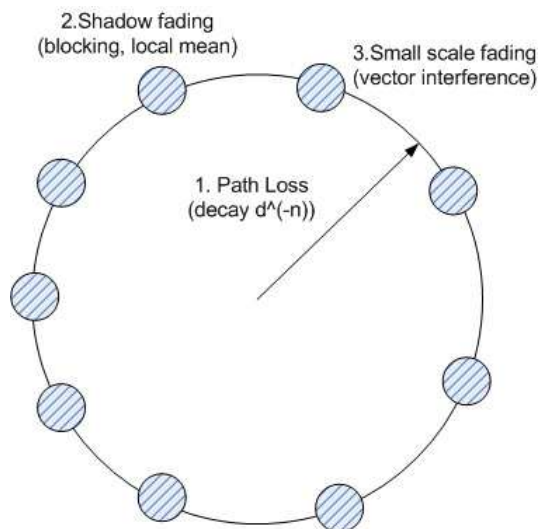### 3.4.1 Pathloss

The large-scale mean of the received power, known as pathloss, depends on the distance between transmitter and receiver. This effect is described in a deterministic manner [16]. Most of the pathloss models have a limitation about the operation frequency, which is generally restricted around 2 GHz. For our purposes, a free-space pathloss model is used for the short-range link. It is used to predict the RSS when the transmitter and the receiver are in conditions of unobstructed LOS between them [17]. As for many other models for large-scale wave propagation, the free-space makes the decay of the signal as function of Transmitter-Receiver separation distance. As explained in [17], the free-space received power is evaluated by the Friis free space equation, specifying that it rate decays of 20dB/decade. When the antennas are assumed to have unity gain, the path loss formula is described as:

$$PL_{dB} = 32.44dB + 10\gamma log_{10}(f) + 10\gamma log_{10}(d) \tag{3.52}$$

where f is the frequency expressed in MHz and d is the distance expressed in km.

3.4.2 Small-Scale Fading

Fast fluctuations of the amplitude of a signal averaged over small distances of the order of a wavelength are represented by small-scale fading. Two different reasons cause these fluctuations.

The first is triggered by the various scatterer elements between the transmitter and the receiver. This fenomenon is called *multipath fading* and it happens when scatterers reflect the electromagnetic signals resulting in out of phase components arriving at the receiver at different delays. Many copies of the transmitted signal, each with different amplitude (A_i), at different phase (θ_i), arrive at different delays (τ_i) [17]. Specifically, if the transmitter sends a unit impulse and there are N scattering elements, the receiver will receive N different delayed versions of the original signal. The channel impulse response is given by the sum of these N scattered versions. The baseband impulse response of a multipath channel can be expressed as [17]:

$$h(t,\tau) = \sum A_i(t,\tau) \exp[j(2\pi f_c \tau_i(t) + \theta_i(t,\tau))]\delta(\tau - \tau_i(t)) \tag{3.53}$$

where $A_i(t,\tau)$ and $\tau_i(t)$ are respectively the real amplitudes and excess delays of the ith multipath component at time t, and f_c is the carrier frequency.

Time dispersive properties are quantified by the mean excess delay ($\overline{\tau}$) and the RMS delay spread (τ_{RMS}). The last is given by the square root of the second central moment ($\overline{\tau^2}$) of the Power Delay Profile (PDP). The PDP contains information about the power from a transmitted delta pulse with a unit energy, which arrives at the receiver with a delay between $[\tau, \tau + d\tau]$, irrespective of a possible Doppler shift [16]:

$$pdp = P_h(\tau) = \int_{-\infty}^{\infty} |h(t,\tau)|^2 dt \tag{3.54}$$

$$\overline{\tau} = \frac{\sum_i P(\tau_i)\tau_i}{\sum_i P(\tau_i)} = \frac{\sum_i A_i^2 \tau_i}{\sum_i A_i^2} \tag{3.55}$$

$$\overline{\tau^2} = \frac{\sum_i P(\tau_i)\tau_i^2}{\sum_i P(\tau_i)} = \frac{\sum A_i^2 \tau_i^2}{\sum_n A_i^2} \tag{3.56}$$

$$\tau_{RMS} = \sqrt{\overline{\tau^2} - (\overline{\tau})^2} \tag{3.57}$$

The second contribution is the *Doppler shift*. It is due to the relative movement between transmitter and receiver, or between scattering elements placed in the channel. Eq. (3.53) shows that the channel impulse response is a function of time t and delay τ. The measure of time variance of a channel is characterized by the maximum doppler frequency (f_m) or doppler spread (f_d). The maximum Doppler frequency is given by $f_m = \frac{v}{\lambda}$, where v is the velocity of the scattering element or the transmitter/receiver and λ is the wavelength of the transmitted signal [17]. If the propagation environment and the surroundings are all static, then the channel transfer function would be a stationary process, i.e., time invariant. However, in practice this is not the case.

Although the literature on dynamic/non-stationary models with time-varying channel parameters is relatively scarce, some models were recently proposed in [18] . These models propose a Tap Delay Line (TDL) Model for BS-MS and MS-MS links in a urban scenario for street-level mobile terminals. As well these models will be adopted for simulations in this report.

Chapter 4

COOPERATIVE MOBILE POSITIONING SYSTEM

The Cooperative Mobile Positioning system is built up by the fusion of two different data types coming from the BSs and the neighboring MSs. The idea behind Cooperative Mobile Positioning originates from the fact that more likely reliable RSS measurements detected among neighboring mobiles can enhance the localization accuracy also in environments where usual terrestrial-based localization techniques offer a bad estimation. This data fusion allows to enhance the localization accuracy in outdoor environments where an OFDM based system is chosen for the long-range link BS-MS and short-range ad-hoc link MS-MS in order to get TDOA and RSS measurements. Fig 5.1 shows the whole implemented simulator for the Cooperative Mobile Positioning. For these investigations we have implemented Mobile WiMAX and WLAN simulator based on IEEE 802.16e and IEEE 802.11a respectively. By performing cross-correlation we can calculate the TDOA values from the Mobile WiMAX simulator, which are the input for the EKF. With these value the EKF can perform the estimate of the user's position.

4.1 WiMAX

In the last few years, the world of telecommunication systems increased he number of broadband subscribers reaching 150 million at the end of 2004. Marketing estimates forecasts that they will reach the number of 350 million in 2008 [19].

Even if wired technologies such as DSL and the optical fibers have covered a fundamental role as leaders in the sector of broadband access, a promising technology such as WiMAX [20] is standing out as a valuable and more efficient alternative,which brings a revolution in transmitting data, video and voice; a greater flexibility in the network's access, and a reduced investment for the infrastructure.

The WiMAX technology is rapidly proposing itself as a new technology able to play an important role in fixed broadband wireless metropolitan area networks [15] also by offering higher data rate and access connectivity from everywhere at low prices. Moreover WiMAX is considered as a strong candidate for 4G and it may be a threat for 3G operators due to its ability in delivering voice and high data speed. Nowadays, providers are trying to decrease the costs of the infrastructure by placing the WiMAX as the preferred standard.

A further characteristic of WiMAX is the flexibility regarding the deployment of the infrastructure by offering Broadband Wireless Access (BWA) by providing different combinations of radio channel types (single carrier vs multicarrier), modulation types, channel coding suitable for fixed, nomadic, portable and mobile services. In a typical cell radius deployment of 3 to 10 kilometers, WiMAX Forum Certified systems can be expected to deliver capacity of up to 40 Mbps per channel, for fixed and portable access applications [22]. Compared to wired technologies, such as DSL, thousands users can be connected with the same speed.

WiMAX completes the Wi-Fi network for wide geographical areas: the MAN and the WAN area network. Fig. 4.1 shows how other technologies have settled in the world of wireless networks. If the WAN is occupied by cellular networks because of their capability to spread the signal over a big area, WiMAX is going to cover both the WAN and MAN areas with other standards such as 3GPP, EDGE, GSM, HiperMAN on one hand, and the 802.20 on the other hand. Instead, in the short-range, Wi-Fi and Bluetooth are technologies that have obtained success in LAN and PAN, respectively.
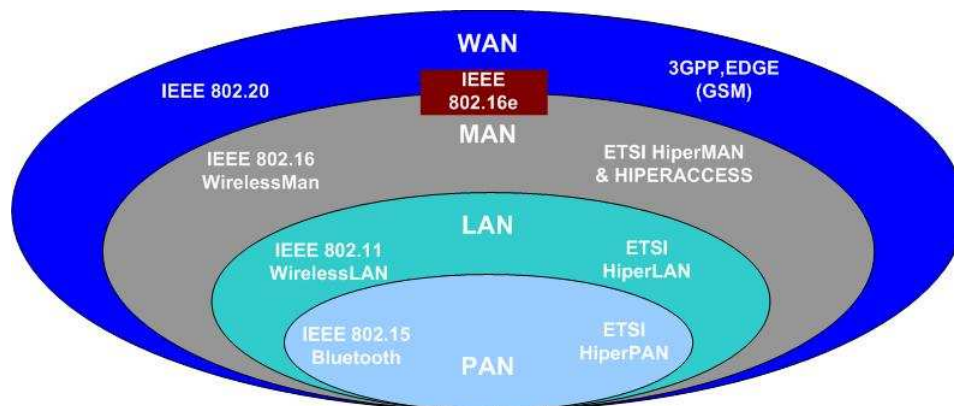

Figure 4.1: Wireless networks coverage area.

WiMAX could provide a connectivity for Wi-Fi APs separated by a long distance with each other. Moreover, in order to increase the coverage and the capacity, the help of WiMAX in connecting Wi-Fi networks in mesh topology can facilitate it.

In fact, a user with portable devices could prefer to be connected to Wi-Fi, when it is available, than WiMAX, since the Wi-Fi card requires less power to transmit the signal

over a short-range. Under this optic the device will choose the fastest connection available at any time.

4.1.1 Inside the Standard: Mobile WiMAX

WiMAX is a set of standards developed by the IEEE 802.16 Working Group. The first version of the standard called 802.16 and released in 2001, was thought for BWA applications. Practically it is designed for LOS scenarios and operates in the 10-66 GHz frequency licensed band. However, neither portability nor mobility are considered and only Point-to-point applications are possible. The next version of the standard, instead, IEEE 802.16-2004, was built to operate in the 2-11 GHz band, thus extending the standard to lower frequency and offering the possibility of connections also in NLOS scenarios. Portability and point-to-multipoint applications were offered in 2003 by IEEE 802.16a first and then by its corrected version IEEE 802.16d in June 2004. Up to this standard, the broadband wireless was only for a fixed infrastructure. Finally, at the end of 2005, the IEEE 802.16e was developed and then published in February, 2006. This is an amendment of the previous standard to permit the access to mobile users as well as the fixed ones, where additional functionalities such as handoff and power saving have been set up to support portable and mobile access together with MIMO and AAS to improve the performance of the system.

The IEEE 802.16-2004 standard together with the IEEE 802.16e standard plus some other mandatory and optional features characterize the Mobile WiMAX Release-1 [15], offering in this manner fixed and mobile network services by meeting the same broadband radio access technology. The Mobile WiMAX Air Interface adopts OFDMA for improved multi-path performance in NLOS environments. Scalable OFDMA (SOFDMA) is introduced in the IEEE 802.16e Amendment to support scalable channel bandwidths from 1.25 to 20 MHz. The Release-1 provides scalability in both radio access and in the architecture. Strong points of Mobile WiMAX are the high data rates, the quality of services, the scalability, the security and of course mobility.

Table 4.1 gives a summary of all the main characteristics of 802.16 technology based both on 802.16-2004 and 802.16e versions. Each technology is characterized by a specific frequency range, scenario, transmission technique, transmission rate corresponding to a given channelization,channel bandwidth and spectrum efficiency, multiple access. The Release-1 defines 2.3, 2.5, 3.3, 3.5 GHz as the possibly frequency bands and 5, 7, 8.75 and 10 MHz as channel bandwidths. Table 4.2 highlights that the 802.16 technology is flexible in deployment because it can use a different frequency band and a different channelization according to the available transmission technique. Both TDD and FDD are supported in the standard [23].

Only the PHY and the MAC layer are defined into the standard. Table 4.2 gives

	802.16-2004	802.16e
Date	June 2004	December 2005
Frequency Bands	2-11 GHz	2-11 GHz/26 GHz
Scenario	LOS/NLOS	LOS/NLOS
Transmission rate	75 Mbps in 20MHz	75 Mbps in 20MHz, 15 Mbps in 5MHz
Multiple Access	OFDM, OFDMA	OFDM, OFDMA, SOFDMA
Duplexing	TDMA, OFDMA	TDMA, SOFDMA
Channel bandwidth	1.25/20 MHz	1.25/20 MHz
Spectrum efficiency	3.75 bps/Hz in 20 MHz	3.75 bps/Hz in 20 MHz, 3 bps/Hz in 5 MHz

Table 4.1: Parameters for 802.16-2004 and 802.16e [23]

WirelessMAN	Applicability	Duplexing	Scenario	Modulation
SC	10-66 GHz	TDD/FDD	LOS	SC
SCa	Below 11 GHz	TDD/FDD	NLOS	SC
OFDM	Below 11 GHz	TDD/FDD	NLOS	OFDM
OFDMA	Below 11 GHz	TDD/FDD	NLOS	OFDMA
HUMAN	Below 11 GHz	TDD		hybrid OFDM/SC

Table 4.2: WiMAX physical layers.

a general overview of the possible physical layers defined. Moreover, the IEEE Working Group after designing the standard and its features also decided to choose a WiMAX open standard in development and application. In this way, it is still possible to guarantee the interoperability with products of different company and other wireless networks. As a result, the consumer will have more benefits in buying these new terminals choosing any operators.

Moreover, it provides important key features necessary for delivering mobile broadband services at vehicular speeds also greater than 120 km/h performing a QoS that has nothing to begrudge to common broadband wireline technologies.

This is possible thanks to an high tolerance to multipath and self-interference, by using orthogonality in subchannels downlink and uplink, scalable channel bandwidths, from 1.25 to 20MHz, Frequency Selective Scheduling, giving the possibility to enhance and optimize the connection quality by taking into account the signal strengths relative to specific users, Power Conservation Management, providing power efficient operations in Sleep and Idle modes, 5 milliseconds Frame Size. An additional key point is that Mobile WiMAX allows diverse economies to realize technologies for specific and diverse geographical environments in order to provide broadband internet access in rural areas and enhancing the capacity of mobile access in suburban and urban areas. Furthermore, the core of the Mobile WiMAX is the mobility. It is this improvement for the fixed WiMAX that can ensure real-time

applications without service degradation also in cases of handover.

Since Mobile WiMAX can provide different types of services, this thesis is focused on the investigation of how the WiMAX technology can tackle the problem of the localization service by using only the available radio signals and without adding any kind of hardware in the WiMAX device.

4.2   Wi-Fi

In late 2001 the WLAN 802.11a technology made its debut into the market providing wireless internet access. It is an OFDM based system very "similar" to the Asymmetrical Digital Subscriber Loop (ADSL), which operates by sending parallel sub-carriers by using the Inverse Fast Fourier Transform (IFFT) and receiving them by using the Fast Fourier Transform (FFT) [24]. The standard specifies an OFDM PHY with 5GHz frequency band splitting signal information into 52 subcarriers, whereas other 802.11 standards specify a 2.4GHz with data rates of 1 and 2 Mbps with Direct Sequence Spread Spectrum (DSSS) or Frequency Hopping Spread Spectrum (FHSS). The 802.11a standard makes use of a pseudo binary sequence by sending it through the pilot subchannel. This can avoid the generation of spectral lines [24]. There are 48 subcarriers to send information in a parallel way providing separates path ways. For a 20MHz subcarrier frequency spacing, 64 subcarrier frequency slots are available. All the subcarriers are mapped with a BPSK, QPSK or QAM modulation and can be sent through 8 channels. Moreover four subcarriers are used as pilots while the other 48 subcarriers are used for carrying data. Each subcarrier is spaced 0.3125 MHz apart [21].

The general characteristics of 802.11a compared to the other WLAN standards 802.11b/g can be summarized as follows:

- Greater scalability;

- Better interferences resistance;

- More users in the same network;

- Higher speed;

- Higher bandwidth applications.

Table 4.3 shows the OFDM parameters for 802.11a.

4.3   System Architecture

In Fig. 2.1 the system architecture is shown. The long-range link (BS-MS) is implemented by using the Mobile WiMAX system parameters. The short-range link (MS-MS) is im-

27

Channel bandwidth	20 MHz
Subcarriers	64
Subcarrier spacing	312,5 kHz
Guard time	0.8 μs
FFT Period	3.2 μs
Symbol rate	4 μs
Modulation	BPSK, 4,16,64 QAM
Data Subcarrier	52
Sampling rate	50 ns

Table 4.3: parameters of OFDM for 802.11a

plemented by using the WLAN 802.11a standard parameters, where an *ad-hoc* network is simulated. As it can be seen, four BSs are taken into account and 2 MSs attached to the same serving BS are the subjects of the investigations. Static and mobile cases are explored. While NLOS conditions are taken into account for each link BS-MS, LOS is considered for the link MS-MS. The channel model implemented is characterized by pathloss and small scale fading.
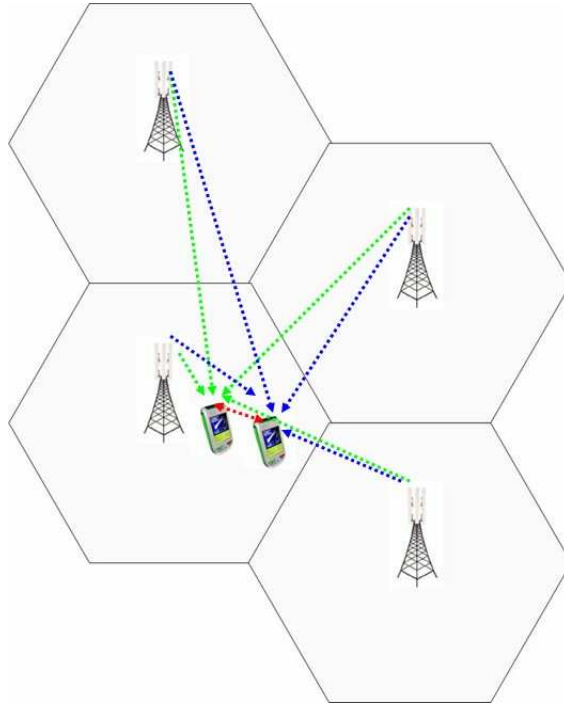

Figure 4.2: System architecture

The proposed localization system is mobile-assisted. In Fig. 4.3 a communication protocol is proposed, where the communication flow starts from a MS that wants to be

localized in an outdoor environment.

As a starting point, the four BSs send to all MSs a sequence of data. Each MS performs the cross-correlation between the arriving signals to estimate the time delay of the incoming packets with respect to the delay of the packets sent by the reference BS being be BS1. As a result, a sets of three TDOA measurements are obtained. Afterwards the MSs start a cooperation process, forming an *ad-hoc* network. One master MS (MS1) and a slave MS (MS2) are assumed, where a packet exchange is carried out with the objective of measuring the power of the received signal between them. In this way, information about their relative distance can be extrapolated. Finally, the slave MS sends its own TDOA measurements to the master MS, which will forward all the collected data to the reference BS. The latter delivers the data to a specific server in the network, which perform the data fusion.

4.4 System Models

4.4.1 BS-MS Links

Physical Layer

Mobile WiMAX PHY is based on OFDM. A block diagram of the OFDM system adopted is depicted in Fig.4.4. Table 4.4 shows the system parameters adopted for the simulations [15].

System Bandwidth (MHz)	5
Carrier Frequency (GHz)	3.5
Sampling Frequency (MHz)	5.6
FFT Size	512
Sub-carrier Frequency Spacing (KHz)	10.94
Useful Symbol Time (us)	91.4
Guard Time (us)	11.4
Symbol Duration (us)	102.9

Table 4.4: Mobile WiMAX parameters for simulations.

Channel Model

When the signal travels from the BS to the MS it is affected by the channel impairments. If in free space scenarios the distance plays a fundamental role in the evaluation of the received signals, in reality several effects have to be taken into account. In our case small
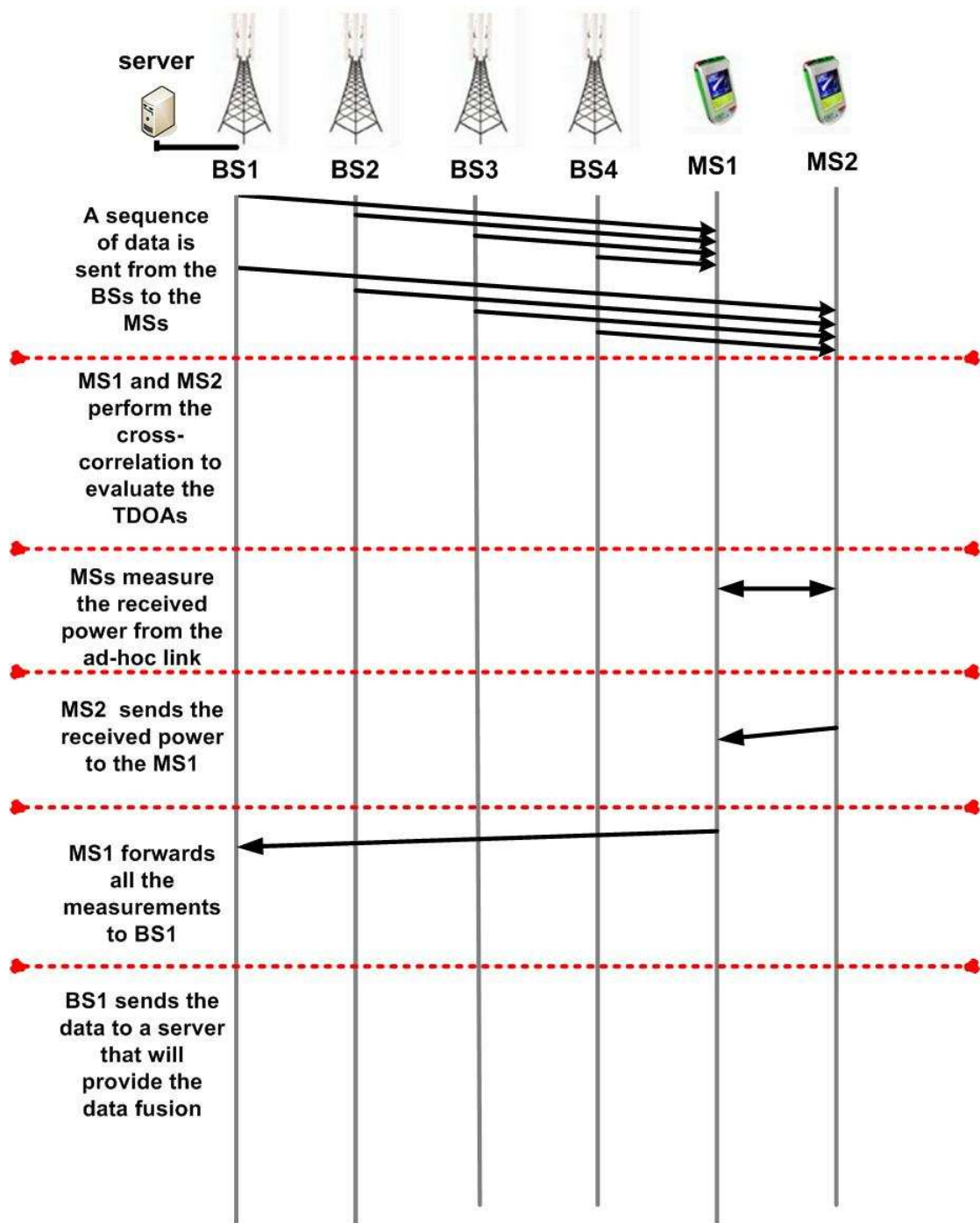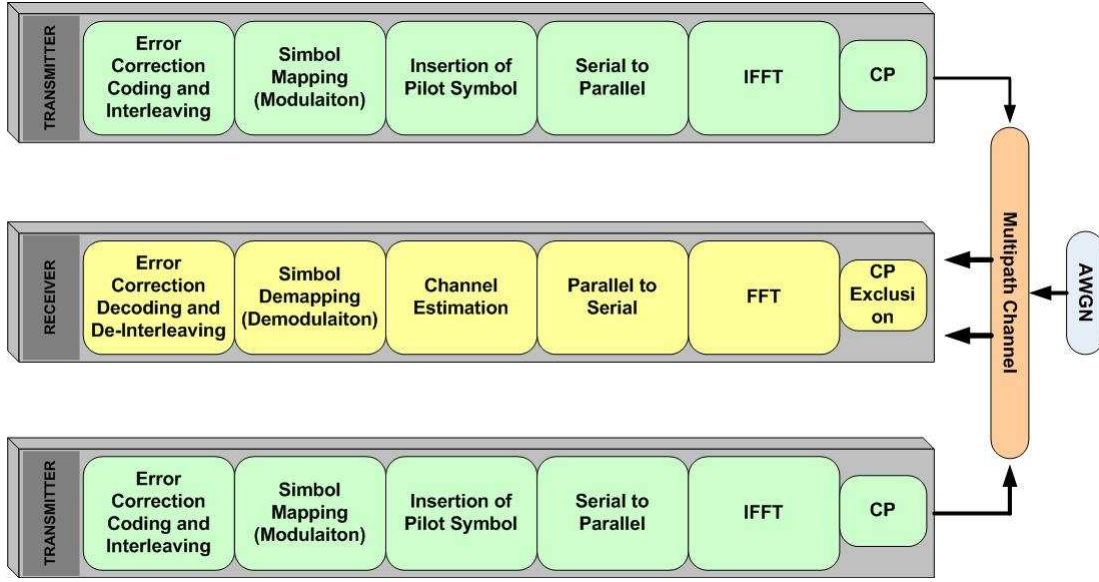
Figure 4.3: Communication Protocol.

Figure 4.4: OFDM System Block Diagram.

scale fading effect is considered. This effect can cause the signal to be delayed before arriving at the receiver. Therefore, a proper model of the channel is needed.

The radio scenario adopted is given by [18], where a NLOS condition for the link BS-MS is considered. A Rayleigh channel is generated according to the Tap Delay Line parameters given by [18] and shown in 4.5

TDOA Measurements

TDOA measurements are calculated by performing cross-correlation between the signals coming from the BSs with respect to the reference BS where the MS is attached. The measurements are done at the receiver (in our case at the MS). As can be seen in Section 4.3 the scenario is composed by four BSs. It means that 3 data sets of TDOA for each MS will be obtained.

Fig. 4.6 shows an example of the performed cross-correlation, where a peak can be clearly recognized where the cross-correlation reaches the maximum value. The peak is in correspondence with the sample index value that represents the estimated delay introduced by the channel model chosen for simulations. A limit in the delay detection by using cross-correlation is given by the sampling time of the system, that according to 4.4 is 175ns. This value represents a lower bound in the channel delay estimation, while the upper bound is given by the delay spread coming out from the tap delay model in Fig. 4.5.

Fig. 4.7 (a) and Fig. 4.7 (b) show the histogram of TDOA values obtained from simulation for BS2-BS3-BS4 with respect to BS1 for MS1 and MS2, respectively. In Fig.

31

Tap index	Delay [ns]	Power [dB]
1	0	-0.5
2	5	0.0
3	135	-3.4
4	160	-2.8
5	215	-4.6
6	260	-0.9
7	385	-6.7
8	400	-4.5
9	530	-9.0
10	540	-7.8
11	650	-7.4
12	670	-8.4
13	720	-11.0
14	750	-9.0
15	800	-5.1
16	945	-6.7
17	1035	-12.1
18	1185	-13.2
19	1390	-13.7
20	1470	-19.8

Figure 4.5: Tap delay model for Mobile WiMAX.

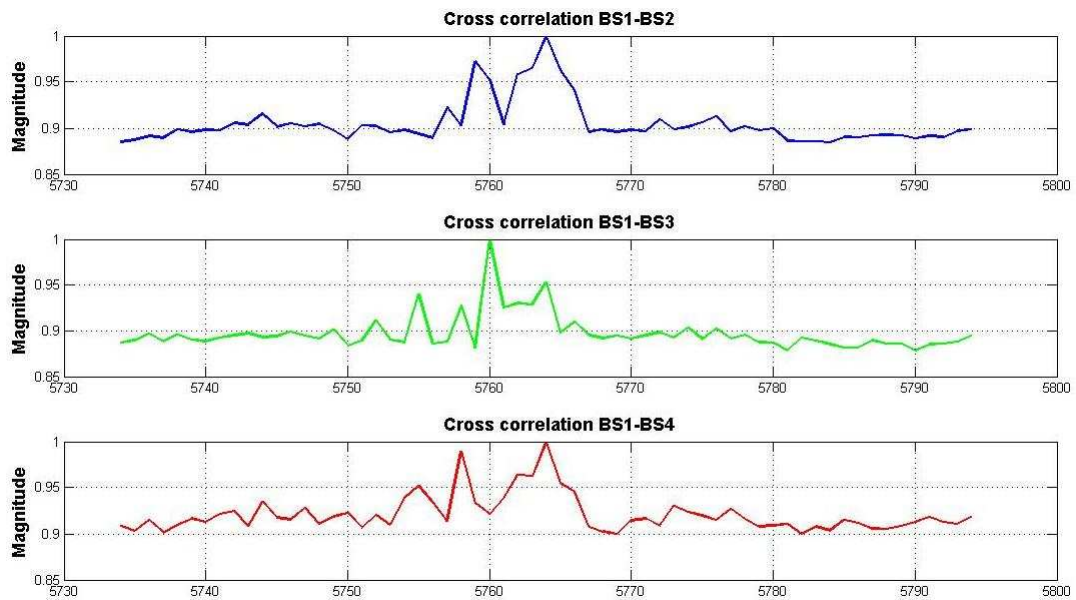Figure 4.6: Cross-correlation for TDOA estimation.

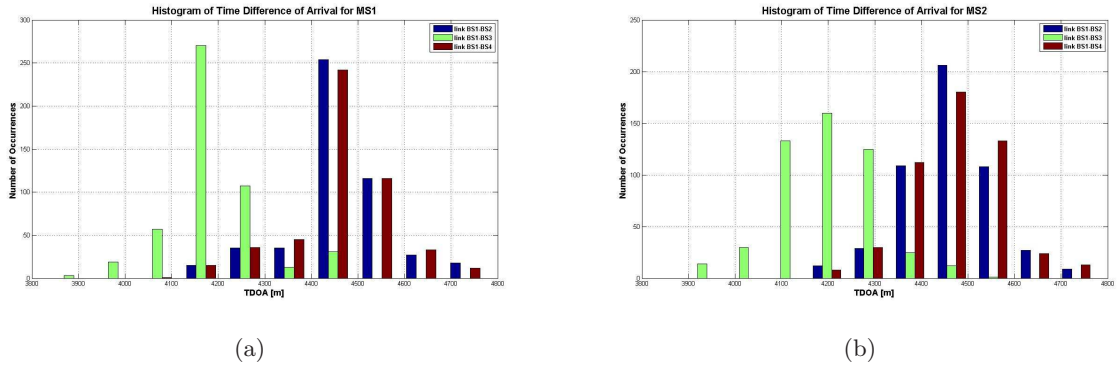(a)   (b)

Figure 4.7: Histogram of TDOA measurements for (a) MS1; and (b) MS2.

4.8 it can be seen that the dispersive delay properties of the channel can introduce errors in distance up to 300m. This value of error is calculated by making the difference between the TDOA calculated by performing the cross-correlation and the real TDOA calculated by multiplying the distance between MS and BSs and subtracting them.
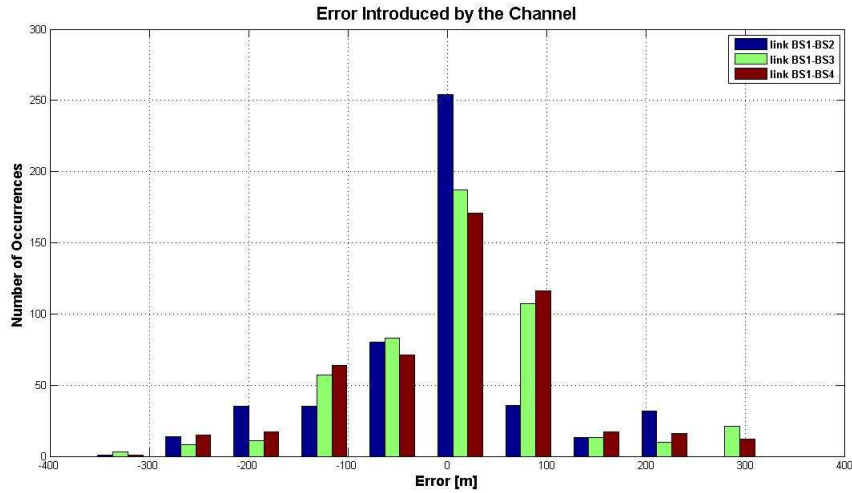

Figure 4.8: Histogram of the error introduced by the channel.

4.4.2   MS-MS link

Physical Layer

WLAN 802.11a is based on OFDM. A block diagram of the OFDM system adopted is depicted in Fig. 3.4. Table 4.5 shows the system parameters adopted for the simulations [25].

Channel bandwidth	20 MHz
Subcarriers	54
Subcarrier spacing	312,5 kHz
Guard time	0.8 μs
FFT Period	3.2 μs
Symbol rate	4 μs
Modulation	BPSK, 4,16,64 QAM
Data Subcarrier	52
Sampling rate	50 ns

Table 4.5: IEEE 802.11a WLAN parameters for simulations.

Channel Model

In the MS-MS link the value measured is the RSS. It is evaluated taking into account the effect of the path loss assumed to be free-space modeled and of the small-scale fading chosen according to Fig.5.6. The simulations are performed by assuming MSs in LOS for this link and a Ricean channel is adopted to implement the effect of multipath.

RSS MEASUREMENTS

RSS measurements are evaluated at the receiver by sending four pilot sub-carriers. At the beginning the power is measured at the transmitter, the average value is evaluated and then the signal is sent through the channel. While the signal travels it is affected by the path loss and the small-scale fading effects. The result is that at the receiver a lower power is measured on the pilots. The difference in dB between transmitted and received power will give the total path loss. Fig. 4.10 shows the histogram of the measured values of loss given by the channel.

4.5 Data Fusion

The core of the Localization System technique is the data fusion. The proposed method is grounded by the fusion of two types of data (TDOA and RSS). This is the reason why it is needed a technique able to perform the fusion of the collected data. As described in the previous chapters the data fusion and the position estimation with and without cooperation is performed by using the EKF.

Several parameters need to be defined to understand how the proposed data fusion can enhance the localization accuracy in positioning and tracking. A distinction has to be done between static and mobile case.

If in the static case the state space is defined as the coordinates of the MSs (Eq. 4.1),

Tap Number	Delay (ns)	Average Relative Power (dB)	Ricean K
1	0	0.0	10
2	10	-10.0	0
3	20	-10.3	0
4	30	-10.6	0
5	50	-6.4	0
6	80	-7.2	0
7	110	-8.1	0
8	140	-9.0	0
9	180	-7.9	0
10	230	-9.4	0
11	280	-10.8	0
12	330	-12.3	0
13	400	-11.7	0
14	490	-14.3	0
15	600	-15.8	0
16	730	-19.6	0
17	880	-22.7	0
18	1050	-27.6	0

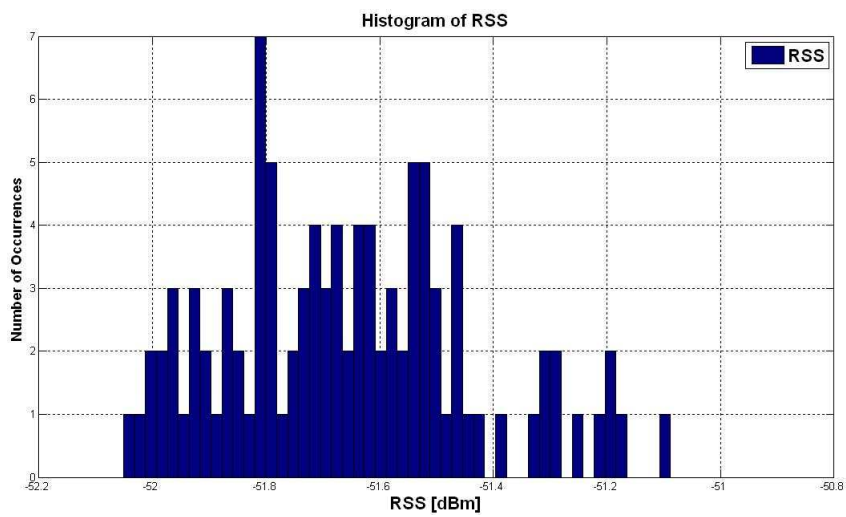Figure 4.9: Tap delay model for WLAN 802.11a.

Figure 4.10: Histogram of RSS values.

in the mobility case it is also defined by the velocity on x and y coordinate (Eq. 4.2). Therefore, the positions' estimators at iteration k are defined as:

$$\hat{\mathbf{x}}_k^{(i)} = \begin{bmatrix} \hat{x}_k^{(i)} & \hat{y}_k^{(i)} \end{bmatrix}^T \qquad (4.1)$$

for the static case, and:

$$\hat{\mathbf{x}}_k^{(i)} = \begin{bmatrix} \hat{x}_k^{(i)} & \hat{vx}_k^{(i)} & \hat{y}_k^{(i)} & \hat{vy}_k^{(i)} \end{bmatrix}^T \qquad (4.2)$$

for the mobility case,

where

$$\hat{\mathbf{x}}_k = \begin{bmatrix} \left\{\hat{\mathbf{x}}_k^{(1)}\right\}^T & \cdots & \left\{\hat{\mathbf{x}}_k^{(n)}\right\}^T \end{bmatrix}^T \qquad (4.3)$$

For the measurements space, $\boldsymbol{\tau}_k^{(i)}$ and $\mathbf{P}_k^{(i)}$ are respectively defined as the set of TDOA and RSS measurements at iteration k of the routine:

$$\boldsymbol{\tau}_k^{(i)} = \begin{bmatrix} \tau_k^{(i)[2]} & \cdots & \tau_k^{(i)[N]} \end{bmatrix}^T \qquad (4.4)$$

$$\mathbf{P}_k^{(i)} = \begin{bmatrix} P_k^{(i)(1)} & \cdots & P_k^{(i)(i-1)} & P_k^{(i)(i+1)} & \cdots & P_k^{(i)(n)} \end{bmatrix}^T \qquad (4.5)$$

The full set of measurements is obtained by grouping all the measurements of the same kind in the same vector:

$$\boldsymbol{\tau}_k = \begin{bmatrix} \left\{\boldsymbol{\tau}_k^{(1)}\right\}^T & \cdots & \left\{\boldsymbol{\tau}_k^{(n)}\right\}^T \end{bmatrix}^T \qquad (4.6)$$

$$\mathbf{P}_k = \begin{bmatrix} \left\{\mathbf{P}_k^{(1)}\right\}^T & \cdots & \left\{\mathbf{P}_k^{(n)}\right\}^T \end{bmatrix}^T \qquad (4.7)$$

and then by compacting all the several types of available measurements in a single vector $\mathbf{z}$, which is given by:

$$\mathbf{z}_k = \begin{bmatrix} \left\{\boldsymbol{\tau}_k\right\}^T & \left\{\mathbf{P}_k\right\}^T \end{bmatrix}^T \qquad (4.8)$$

The last step is the determination of the process and measurements noise covariance matrices (see Eq. (4.9) and Eq. (4.10)).

In order to allow a faster convergence of the filter, $\mathbb{Q}$ is defined as a diagonal matrix with values of some order smaller than the expected values of the states:

$$\mathbb{Q} = \sigma_{xy}^2 \mathbb{I}, \quad \sigma_{xy} \ll \hat{x} \vee \hat{y} \qquad (4.9)$$

For the measurements noise, $\mathbb{R}$ is defined as a diagonal matrix (no correlation between measurements), which is given by:

$$\mathbb{R} = \begin{bmatrix} \sigma_\tau^2 \mathbb{I} & 0 \\ 0 & \sigma_p^2 \mathbb{I} \end{bmatrix} \qquad (4.10)$$

where $\mathbb{I}$ is an identity matrix of appropriate dimensions, and σ_τ^2 and σ_p^2 are directly derived from the available measurements:

$$\sigma_\tau^2 = \left[\begin{array}{ccccccc} \sigma_{\tau(1)[1]}^2 & \cdots & \sigma_{\tau(1)[N]}^2, & \ldots, & \sigma_{\tau(n)[1]}^2 & \cdots & \sigma_{\tau(n)[N]}^2 \end{array} \right]^T \tag{4.11}$$

$$\sigma_p^2 = \left[\begin{array}{ccccccc} \sigma_{P(1)(2)}^2 & \cdots & \sigma_{P(1)(n)}^2, & \ldots, & \sigma_{P(n)(1)}^2 & \cdots & \sigma_{P(n)(n-1)}^2 \end{array} \right]^T \tag{4.12}$$

Assuming for simplicity to consider only additive white gaussian noise, the matrices $\mathbb{W}_k$ and $\mathbb{V}_k$ are equal to the identity matrix $\mathbb{I}$, regardless the iteration k. The matrices $\mathbb{A}_k$ and $\mathbb{H}_k$ represent the Jacobian of Eq. (4.1) and Eq. (4.2) with respect to $\mathbf{x}_k$.

If MSs are static, $\mathbb{A}_k$ is equal to the identity matrix $\mathbb{I}$. Different is the case of mobility where $\mathbb{A}_k$ is equal to:

$$A = \begin{pmatrix} 1 & 0 & T & 0 \\ 0 & 1 & 0 & T \\ 0 & 0 & 1 & 0 \\ 0 & 0 & 0 & 1 \end{pmatrix}$$

Chapter 5

SIMULATION RESULTS

This chapter focuses on the analysis of the results obtained for static and mobile cases. Computer simulations have been performed in order to compare the location estimation accuracy of the Cooperative Mobile Positioning with the one estimated without.

5.1 Simulator Block

A block diagram of the whole simulator is shown in Fig. 5.1 and the procedure implemented in the various blocks can be summarized as follows:
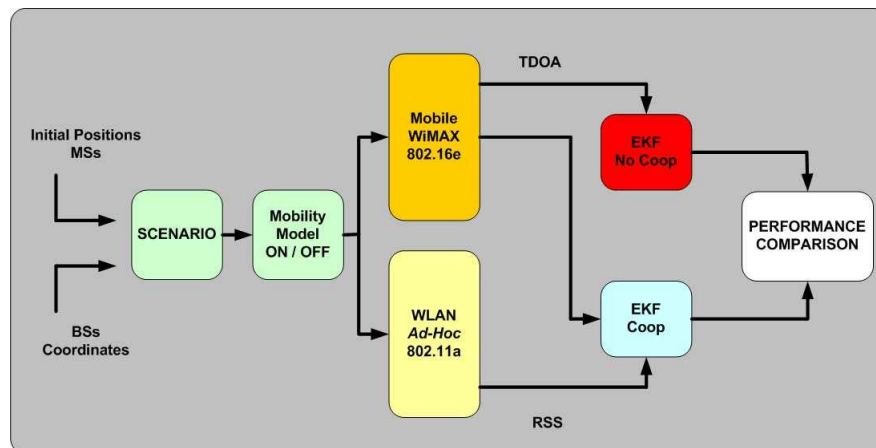

Figure 5.1: Simulator: block diagram.

- Scenario: It is created by defining the initial positions of the MSs and the coordinates of the BSs.

- Mobility Model:It is static or dinamic for both MSs.

- Mobile WiMAX: A simulated TDOA measurements are calculated according to the instantaneous positions of the MSs obtained in the Mobility Model block.

- WLAN: A WLAN 802.11a system is simulated and RSS measurements are calculated according to the relative distances between the MSs.

- EKF No Coop: The EKF is implemented and the estimate of the MSs' position are evaluated if users are in static conditions. A tracking of the path of the users is performed in mobility conditions, instead Cooperation is not applied.

- EKF Coop: The EKF is implemented by combining the TDOA and the RSS measurements. The estimate of the MSs' positions are evaluated if users are in static conditions. A tracking of the path of the users is performed in mobility conditions, instead Cooperation is applied.

- Performance Comparison: An evaluation by comparing the results obtained with and without cooperation is done.

5.2   Static Case

Simulations for the static case are carried out in a cell of radius 3 km, where MS_1 and MS_2 are placed in (500,10) and (500,-10), respectively. Two hundred sets composed of two hundred measurements of TDOA and RSS values are simulated to obtain a distribution of the estimated positions. Note that the number of measurements needed for obtaining a location estimate plays an important role in the EKF performance; after several investigations it has been observed that two hundred measurements are enough to make the filter converge. Fig. 5.2 shows an example of the convergence of the EKF filter in the x coordinate and y coordinate estimate inherent to MS1 for cooperative (red line) and non cooperative case (blue line). It can be already observed that the cooperation enhances the localization accuracy by making the filter converging to an estimation closer to the real value.

Fig. 5.3 and Fig. 5.4 show the results achieved for both MS_1 and MS_2. The small blue and red crosses represent the positions estimated by the EKF for the non-cooperative and the cooperative case, respectively. The big crosses, instead, are the mean values of all the estimates. It is evident that cooperation brings down the average root mean square error (RMSE)[1], as each of the two mean estimates are closer to the real positions in case of cooperation. In order to ascertain this benefit, the cumulative distribution function (CDF) of the average RMSE for MS_1 is plot in Fig. 5.3 and Fig. 5.4.

---

[1]The Root Mean Square Error (RMSE) is defined as:

$$RMSE = \sqrt{(X_{real} - X_{est})^2 + (Y_{real} - Y_{est})^2} \tag{5.1}$$

Figure 5.2: An example of the convergence of the filter (a) for coordinate x; and (b) for coordinate y.

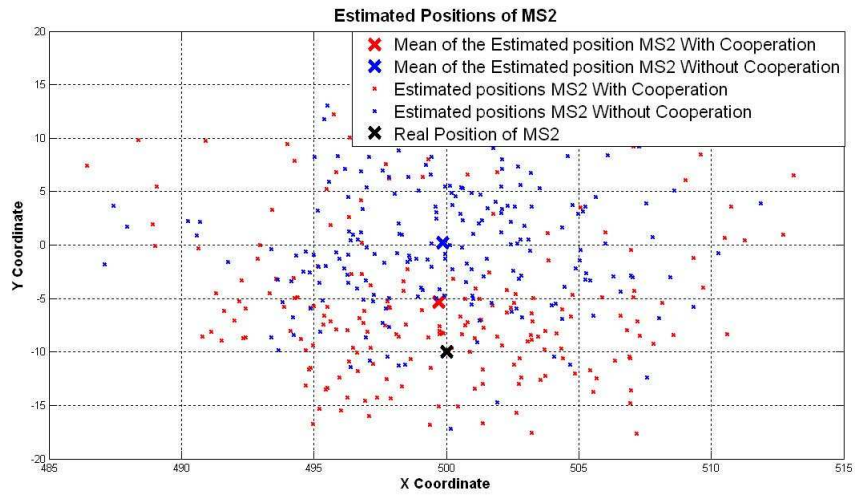Figure 5.3: Estimated positions for MS1.

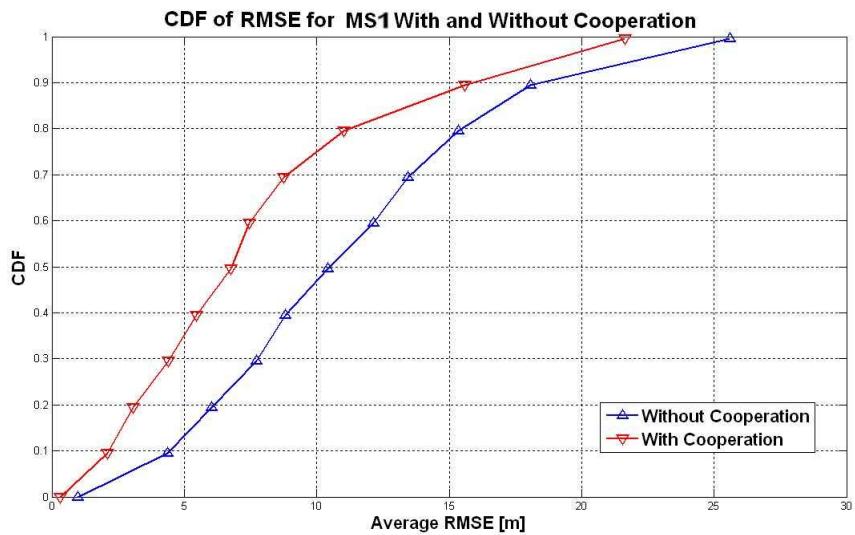Figure 5.4: Estimated positions for MS2.
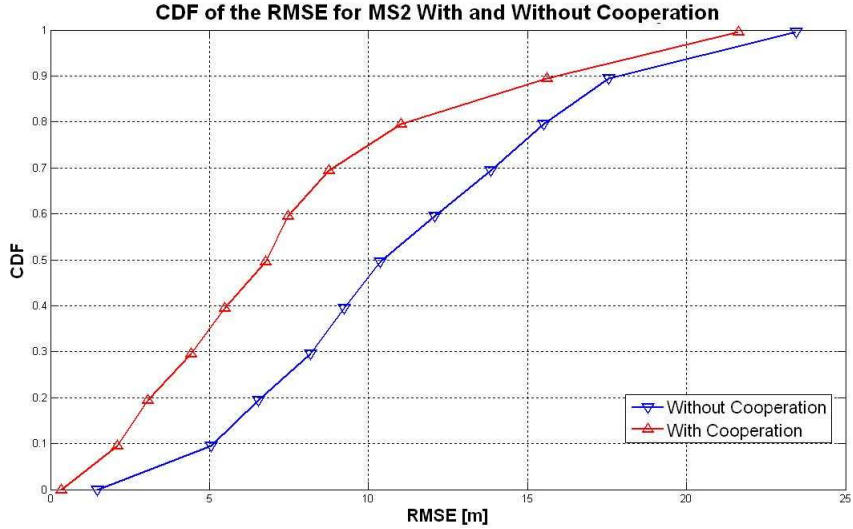

Figure 5.5: CDF of RMSE for MS1.

Figure 5.6: CDF of RMSE for MS2.

5.3 Dynamic Case

As in 5.2 results are reached in case of mobility. Different kind of situations have been simulated. Specifically, long path movements with direction-changing are investigated in a urban environment where NLOS conditions for MS-BS links and LOS conditions for MS-MS links are assumed. In order to focus on the benefit and the limits of cooperation, pedestrian movement at 3 km/h is considered. Since the users are moving, different factors affecting the channel conditions, such as doppler spread, are considered in the simulations.

### 5.3.1 *Scenario 1*: Parallel walking

Fig. 5.7 (a) shows the chosen road for the path and the reciprocal configuration of the users. Initial parameters are mentioned in Table 5.3.1. Fig. 5.7 (b) and 5.7 (c) show the estimated path for MS1 and MS2 respectively with and without cooperation. Table 5.3.1 shows the average RMSE evaluated through the estimated path. It results under the models assumed to simulate the system that cooperation reduces the average RMSE of about **26%** for both mobiles.

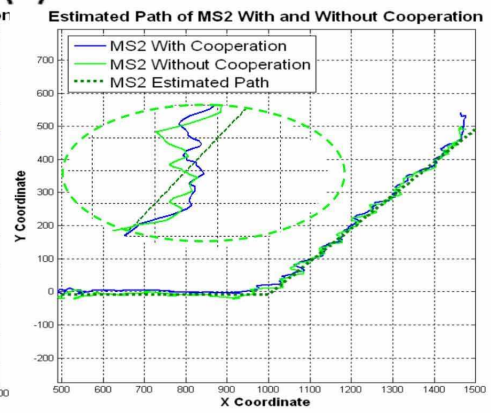Table 5.1: Configuration parameters for *scenario 1*.

MS1 Coordinate	(500 , 10)
MS2 Coordinate	(500 , -10)
Distance between Mobiles	20 m
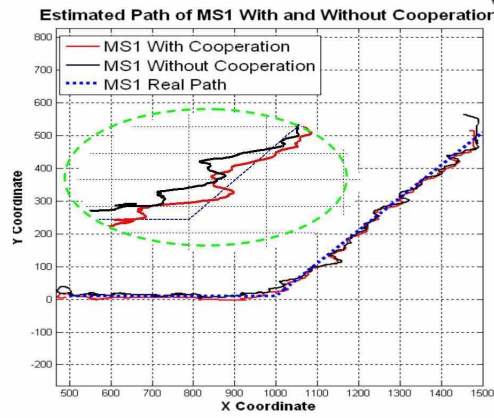
Figure 5.7: Tracking for scenario 1.

Table 5.2: Average RMSE for case 1.

	Mean	Standard Deviation	Gain
RMSE MS1 Without Cooperation	42.62 m	22.69 m	
RMSE MS1 With Cooperation	31.25 m	15.92 m	
RMSE MS2 Without Cooperation	40.42 m	22.35 m	
RMSE MS2 With Cooperation	29.69 m	15.60 m	

Table 5.3: Gain for scenario 1.

MS1 Gain [%]	22.6
MS2 Gain [%]	9.6

5.3.2 *Scenario 2*: Follow-Man Walking

In this situation users are moving first as in the previous case, then after five hundred meters they change direction starting to walk one behind the other. Fig. 5.7 (a) shows the chosen road for the path and the reciprocal configuration of the users. Initial parameters are mentioned in Table 5.3.1. Fig. 5.8 (b) and 5.8 (c) show the estimated path for MS1 and MS2 respectively with and without cooperation, whereas Table 5.3.2 shows the average RMSE evaluated through the estimated path. Same result as before: under the models assumed to simulate the system, cooperation reduces the average RMSE of about **22%**.

Table 5.4: Configuration parameters for *scenario 2*.

MS1 Coordinate	(500 , 10)
MS2 Coordinate	(500 , 0)
Distance between Mobiles	10 m

Table 5.5: Average RMSE for scenario 2.
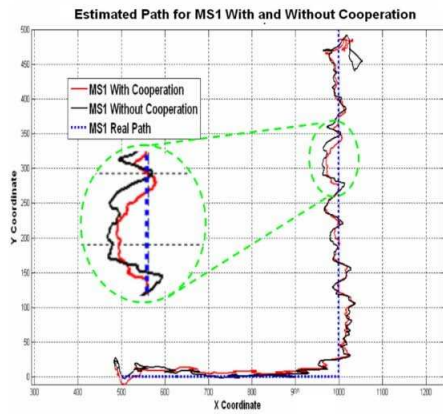
	Mean	Standard Deviation
RMSE MS1 Without Cooperation	44.61 m	24.71 m
RMSE MS1 With Cooperation	34.56 m	18.77 m
RMSE MS2 Without Cooperation	42.13 m	22.35 m
RMSE MS2 With Cooperation	33.95 m	18.49 m

Table 5.6: Gain for case 2.

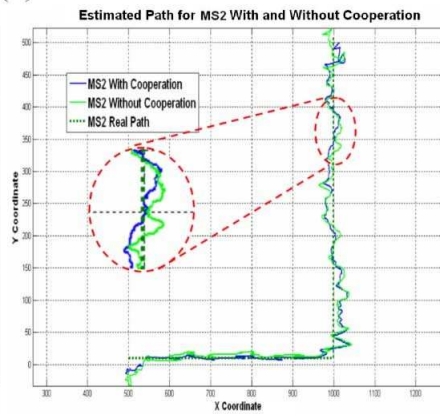| MS1 Gain [%]	22.6
MS2 Gain [%]	9.6

(a)

(b)

(c)

Figure 5.8: Tracking for scenario 2.

5.3.3 *Scenario 3*: Diverging Walking

A different approach has been taken in scenario 3, where users walking to diverging directions have been simulated. Initial configuration is stated in Table 5.3.3

Table 5.7: Configuration parameters for *scenario 3*.

MS1 Coordinate	(500 , 10)
MS2 Coordinate	(500 , -10)
Distance between Mobiles	20 m (*increasing*)

Fig 5.9 show the estimated path for the two users. Since the measurements have been done with a step of one second with a velocity of 1m/s and the total path is 1500 meters we have collected a set of 1500 measurements. During the first 500 steps (500 m) the distance between the users is enough to have good measurements of RSS from the *ad-hoc* link as in the previous cases. After 500 meters the users change directions and start to follow different paths. The distance between them starts to increase and different values of RSS start to be detected by the users. As it is expected, after some steps the cooperation starts to loose its influence. In order to explain the phenomenon Fig. 5.10 shows the instantaneous RMSE evaluated through the path with and without cooperation. If during the first 500 steps the RMSE with cooperation (red line) is lower compared to the case without cooperation (blue line), after 500 steps (when the two users have changed direction) the evaluated RMSE with cooperation starts to overlap the one obtained without until they become almost the same. A better overview is given in Table 5.3.3 where the mean value of the RMSE has been calculated for the steps 1-500 , 501-1000, 1001-1500. Thus Table 5.3.3 shows the gain for the relative steps.
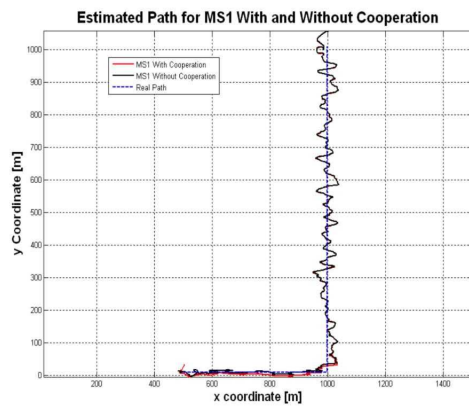
Table 5.8: Average RMSE for scenario 3.

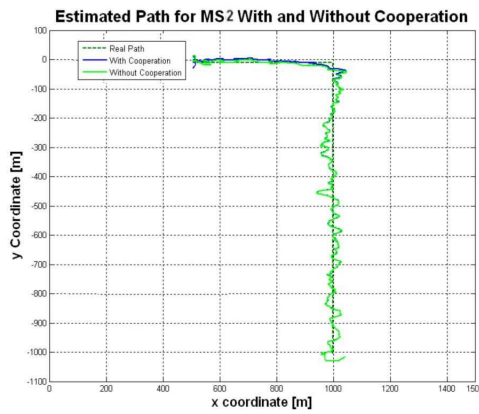| STEPS	1:500	501:1000	1001:1500
RMSE MS1 Without Cooperation	41.62 m	43.98 m	42.56m
RMSE MS1 With Cooperation	33.05 m	43.11 m	42.50m
RMSE MS2 Without Cooperation	40.42 m	43.98 m	37.56m
RMSE MS2 With Cooperation	31.48 m	43.33 m	37.55m

Table 5.9: Gain for scenario 3.

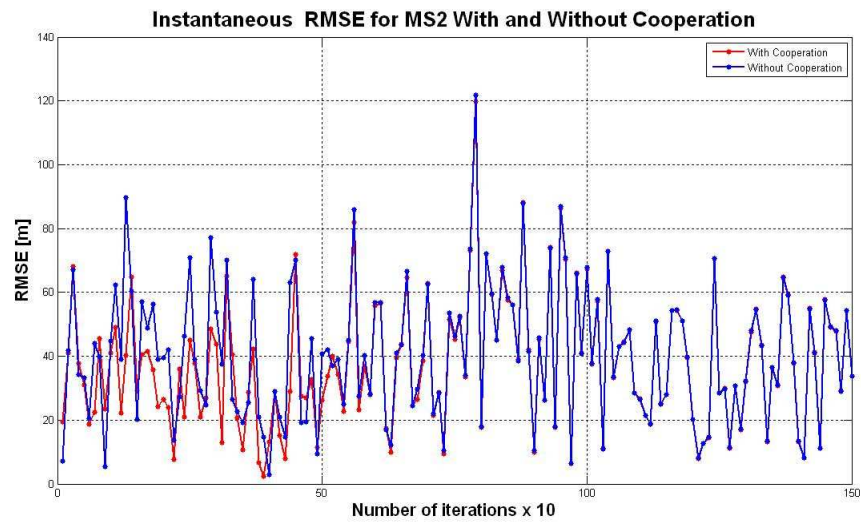| STEPS	1:500	501:1000	1001:1500
MS1 Gain [%]	20.6	1.9	0.1
MS2 Gain [%]	22.2	1.4	0.02

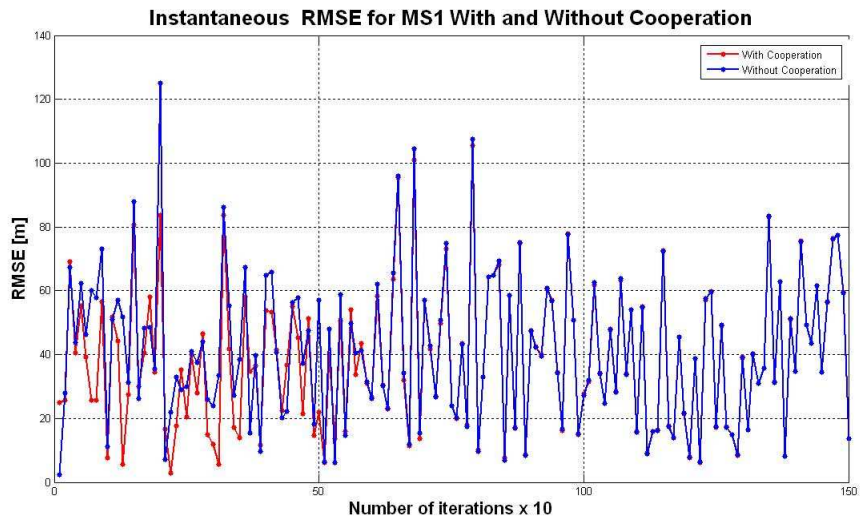Figure 5.9: Tracking for scenario 3.

Figure 5.10: Instantaneous RMSE with and without cooperation.

Chapter 6

CONCLUSIONS AND FUTURE WORK

In this thesis, we have proposed an innovative solution for positioning and tracking estimation in hybrid 4G wireless networks by introducing the Cooperative Mobile Positioning System (COMET). The graphical and numerical results shown in the chapter have demonstrated that, regardless the cooperation enhances the location estimation accuracy with respect to conventional non cooperative positioning techniques in stand-alone cellular networks. Hence, this work has demonstrated that the emerging paradigm of wireless cooperation has a beneficial impact on wireless location.

6.1 Future Work

The future work will be focused on the creation of a scalability algorithm enabling clustering in the proposed tracking scenario. Additionally, more complex individual and group mobility models will be investigated, where different velocities will be considered to account the pedestrian as well as the vehicular case.

Bibliography

[1] A.H. Sayed,A. Tarighat, N. Khajehnouri *Network-Based Wireless Location: Challenges Faced in Developing Techniques for Accurate Wireless Location Information* IEEE Signal Processing Magazine, July, 2005, Vol. 22; No. 4; pp. 24-40.

[2] *User Equipment (UE) positioning in Universal Terrestrial Radio Access Network (UTRAN)*, (3GPP TS 25.305 version 7.3.0 Release 7) ETSI TS 125 305 V7.3.0 (2006-06);

[3] Frattasi S, Fathi H, Fitzek FHP, Katz M, Prasad R. *Defining 4G Technology From the User Perspective.* IEEE Network Magazine, January-February, 2006, Vol. 20; No. 1; pp. 35-41.

[4] *White Paper WiMAX Forum 24 September*, 1 October 2006 Bechtel Labs, Frederick,MD,USA.

[5] S. J. Vaughan-Nichols, *Achieving wireless broadband with wimax* IEEE Computer, vol. 37, no. 6, pp. 10 13, 2004.

[6] *K. R. S. G. S. Kumaran, Migration to 4 g: Mobile ip based solutions*, AICT-ICIW 06, vol. 00, pp. 76 76, 2006.

[7] Muhammad Aatique, MASTER THESIS, *Evaluation Of Tdoa Techniques For Position Location In CDMA Systems.* Virginia Polytechnic Institute and State University September 1997

[8] A. Mordechai, D. Hertz, *Time Delay Estimation by Generalized Cross Correlation Methods*, IEEE TRANSACTIONS on acoustics, speech, and signal processing, VOL. ASSP-32, NO. 2, APRIL 1984

[9] B.Ristic, S.Arulampala, M. N.Gordon. *Beyond the Kalman filter*, Boston: Artech House, 2004.

[10] R.G.Brown, P.Y.C. Hwang. *Introduction To Random Signals And Applied Kalman Filtering. With Matlab Exercises And Solutions*, New york: John Wiley and Sons, 1997.

[11] R.E.Kalman. *A New Approach To Linear Filtering And Prediction Problems*, Trans. AMSE-J. Basic Eng., 35-45, March 1960.

[12] M.S.Grewal, A.P.Andrews *Kalman Filtering: Theory and Practice*, Prentice Hall, 1993.

[13] D.Fox, J.Hightower, L.Liao, D.Shulz, G.Borriello. *Bayesian Filtering For Location Estimation* paper. University of Washington.

[14] G.Welsh, G.Bishop. *An Introduction to the Kalman Filter*, TR 95-041, Department of Computer Science, University of North Caroline at Chapel Hill, July 2006.

[15] WiMAX Forum *Mobile WiMAX Part I: A Technical Overview and Performance Evaluation*, August 2006.

[16] A.F. Molisch *Wireless Communications* IEEE Press, Wiley, England, 2005.

[17] T.S. Rappaport, *Wireless Communications: Principles and Practice*, Prentice Hall PTR; 2nd edition, December 31, 2001.

[18] IEEE 802.16j Relay Task Group, *Channel Models and Performance Metrics for IEEE 802.16j Relay Task Group*, 2006-05-01.

[19] F. Behmann, *Impact of Wireless (Wi-Fi, WiMAX) on 3G and Next Generation An Initial Assessment.*

[20] *"www.wimaxforum.org"* 20 December 2006.

[21] M.S.Gast, *802.11 Wireless Networks: The Definite Guide.* O'Really, Appril 2002.

[22] White Paper, Mobile WiMAX Plugfest, September-October 2006, Frederick, MD, USA.

[23] WiTech, *Tutorial on WiMAX technologies*, June 2006.

[24] 802.11a White Paper, VOCAL Technologies, Ltd.Home Page.

[25] J. Medbo, J.E. Berg, *Measured Radiowave Propagation Characteristics at 5 GHz for typical HIPERLAN/2 Scenarios*, ETSI EP BRAN ,30

March1998.